Investigational New Drugs **17:** 343–359, 1999.

Invited Review

Orthotopic metastatic mouse models for anticancer drug discovery and evaluation: a bridge to the clinic

Robert M. Hoffman
AntiCancer, Inc., San Diego, CA, USA

Key words: metastasis, surgical orthotopic implantation, immunodeficient mice, green fluorescent protein, tumor imaging, clinically-relevant models

Summary

Currently used rodent tumor models, including transgenic tumor models, or subcutaneously-growing human tumors in immunodeficient mice, do not sufficiently represent clinical cancer, especially with regard to metastasis and drug sensitivity. In order to obtain clinically accurate models, we have developed the technique of surgical orthotopic implantation (SOI) to transplant histologically-intact fragments of human cancer, including tumors taken directly from the patient, to the corresponding organ of immunodeficient rodents. It has been demonstrated in 70 publications describing 10 tumor types that SOI allows the growth and metastatic potential of the transplanted tumors to be expressed and reflects clinical cancer. Unique clinically-accurate and relevant SOI models of human cancer for antitumor and antimetastatic drug discovery include: spontaneous SOI bone metastatic models of prostate cancer, breast cancer and lung cancer; spontaneous SOI liver and lymph node ultra-metastatic model of colon cancer, metastatic models of pancreatic, stomach, ovarian, bladder and kidney cancer. Comparison of the SOI models with transgenic mouse models of cancer indicate that the SOI models have more features of clinical metastatic cancer. Cancer cell lines have been stably transfected with the jellyfish *Aequorea victoria* green fluorescent protein (GFP) in order to track metastases in fresh tissue at ultra-high resolution and externally image metastases in the SOI models. Effective drugs can be discovered and evaluated in the SOI models utilizing human tumor cell lines and patient tumors. These unique SOI models have been used for innovative drug discovery and mechanism studies and serve as a bridge linking pre-clinical and clinical research and drug development.

Abbreviations: SOI, surgical orthotopic implantation, GFP, green fluorescent protein, G418, geneticin, 5-FU, 5-fluorouracil, SCLC, small cell lung cancer

Introduction

A. Background of surgical orthotopic implantation (SOI) mouse models of human cancer

In the past 10 years, we have developed a new approach to the development of a clinically-accurate rodent model for human cancer based on our invention of surgical orthotopic implantation (SOI). The SOI models have been described in approximately 70 publications [1–71] and in four patents[1]. SOI allows human tumors of all the major types of human cancer to reproduce clinical-like tumor growth and metastasis in the transplanted rodents [1–71]. The major features of the SOI models are reviewed here and also compared to transgenic mouse models of cancer.

[1] U.S. Patent Nos. 5,569,812 and 5,491,284; European Patent No. 0437488; Japanese Patent No. 2664261.

B. Previous in vivo screening systems

1. *Early screening systems*. Early screening *in vivo* systems for drug discovery included the L1210 mouse leukemia [72]. A more sensitive mouse leukemia, P388, was introduced somewhat later [73]. The possibility of more relevant screening was expanded when

Rygaard utilized the newly-isolated athymic nude mouse to transplant human tumors [74]. Screening with human xenografts started with the colon CX-1, lung LX-1 and breast MX-1 tumors [75]. The U.S. National Cancer Institute (NCI) and the Central Institute of Experimental Animals of Japan have greatly expanded the number of human tumor cell lines which can grow in nude mice. However the early nude mouse models were quite distinct from clinical cancer. The human tumors were implanted subcutaneously, which is a very different micro-environment from the tissue of origin of the tumors. The subcutaneous environment usually precludes the tumors from metastasizing. Workers such as Sordat and Fidler [76] have partly addressed this point, by introducing orthotopic transplantation of suspensions of tumor cell lines in nude mice as detailed below.

2. *Orthotopic injection of suspensions of established cell lines*. Fidler [76] noted that the subcutaneous micro-environment for human visceral tumors is very different from their original milieu. He postulated that this difference may result in the lack of metastases and the altered drug responses seen in the subcutaneous models. Indeed radical differences have been noted by Fidler [77] and us [20] in the drug responses of tumors in the orthotopically-transplanted site vs. the tumor growing subcutaneously. Despite species difference, the corresponding nude mouse organ more closely resembles the original patient micro-environment than the subcutaneous milieu.

Injecting tumor cell suspensions into the analogous or orthotopic mouse sites occasionally allowed relevant metastases. For example, disaggregated human colon-cancer cell lines injected into the cecum of nude mice produced tumors that eventually metastasized to the liver [76]. Although orthotopic injection of cell suspensions is an improvement over simple subcutaneous implantation, the technique has several major drawbacks. Orthotopic cell injection so far has been shown to work essentially only with established cell lines which greatly restricts its utility. The tumors resulting from orthotopic transplantation of cell suspensions often showed relatively low rates of metastasis compared to the original tumor in the patient and to SOI [1–71].

C. Surgical orthotopic implantation (SOI) of tumor fragments

The SOI models circumvent the cell disaggregation step used in previous orthotopic models. Instead of injecting cell suspensions into the orthotopic site, we have developed micro-surgical technology to transplant tumor fragments orthotopically [1–71]. The development of SOI technology led to a profound improvement in the results achieved in that the metastatic rates and sites in the transplanted mice reflect the clinical pattern after SOI. The advantages of SOI appear quite general having been seen in comparison to orthotopic implantation of cell suspensions for bladder [2,3], lung [4,9,10,24,26,27], stomach [5,14,18], kidney [78], and colon cancers [1,6,8,16,32,66–70].

In a head-to-head comparison of SOI with orthotopic transplantation of cell suspensions, SOI of stomach cancer tissue fragments resulted in metastases in 100% of the nude mice with extensive primary growth. Metastases were found in the regional lymph nodes, liver, and lung as is characteristic of this cancer [5]. In contrast, orthotopic injection of suspensions of stomach cancer cells to the nude-mouse stomach resulted in lymph node metastases in only 6.7% of those mice bearing tumors and no distant metastases.

We also compared the metastatic rate of human renal cell carcinoma SN12C in the two orthotopic nude mouse models [78] SOI of tumor tissue and orthotopic injection of cell suspensions in the kidney. The primary tumors resulting from SOI were larger and much more locally invasive than primary tumors resulting from orthotopic transplantation of cell suspension. SOI generated higher metastatic rates than orthotopic transplantation of cell suspensions. The differences in metastatic rates in the involved organs (lung, liver, and mediastinal lymph nodes) were 2–3 fold higher in SOI compared to orthotopic transplantation of cell suspensions ($p < 0.05$). Median survival time in the SOI model was 40 days, which was significantly shorter than that of orthotopic transplantation of cell suspensions (68 days) ($p < 0.001$). Histological observation of the primary tumors from the SOI model demonstrated a much richer vascular network than the orthotopic transplantation of cell suspension. Lymph node and lung metastases were larger and more cellular in the SOI model compared to the orthotopic transplantation of cell suspension models.

We conclude that the tissue architecture of the implanted tumor tissue in the SOI model plays an important role in the initiation of primary tumor growth,

invasion, and distant metastasis. These studies directly demonstrate that the implantation of histologically intact tumor tissue orthotopically allows accurate expression of the clinical features of human cancer in nude mice. Experiments showed that distant tumor growth in the SOI models were true time-dependent metastases resulting from clinical-like routes and not due to cells shed in transplantation [17]. Thus the SOI models are a significant improvement allowing the full metastatic potential of human tumors to be expressed in a rodent model. A limitation to the SOI technique is the high level of surgical skill necessary for the implantation procedures.

D. Drug discovery with SOI models

The antitumor and antimetastatic efficacy of the following new agents have been demonstrated in SOI models:

1) The metalloproteinase inhibitor Batimastat: Found to be active against an SOI human-patient colon tumor model [28] including:
   a. inhibition of primary tumor growth
   b. inhibition of metastatic events,
   c. extension of survival.
2) The metalloproteinase inhibitor CT1746: Found to be active against an SOI human colon tumor xenograft model [79] including:
   a. arrest of primary tumor growth
   b. inhibition of metastatic events, and
   c. a large increase in survival.
3) IFN-γ: Found to be active against a patient pleural cancer SOI model [45] including:
   a. elimination of metastatic events
   b. decrease in cachexia, and
   c. extension of survival.
4) Angiogenesis inhibitor TNP-470: Found to be active in patient colon and stomach tumor SOI models [66–70] including:
   a. inhibition of liver metastasis in colon cancer
   b. minimal or no effect on primary tumor

Feasibility for the drug discovery in the SOI models has been demonstrated with colon, pancreatic, stomach and lung cancer whose chemotherapy has resulted in dose-response, differential sensitivity of primary and metastatic tumors, reproducibility and correlation to historical clinical activity of the drugs [16,18–20,22–26,28,66–71]. Ongoing clinical studies with the new agents listed above will provide further correlative information.

E. Discovery of basic aspects of metastasis and possible new therapeutic targets

It was shown with the SOI colon cancer models that liver colonization is the governing process of colon cancer liver metastasis [32]. This study further confirmed Paget's seed and soil hypothesis and demonstrated that the liver colonization event is a potential therapeutic target to prevent metastasis.

We have developed a new antimetastatic chemotherapeutic strategy for combination with hepatic resection of human colon cancers in nude mice. The procedure involves i.p. administration of 5-FU two hours before hepatic resection of the colon tumors. Therapy was then continued for four consecutive days. We termed this strategy neo-neoadjuvant chemotherapy. The regime was tested in the AC3488 nude mice model of highly malignant human colon cancer [62] and significantly prolonged animal survival compared to 5-FU adjuvant chemotherapy; surgery alone; 5-FU without surgery; or the untreated control. The 5-FU neo-neoadjuvant chemotherapy had a 50% survival of 68 days compared to 41 days for 5-FU neo-adjuvant treatment; 32 days for 5-FU adjuvant therapy; 30 days for surgery only; 28 days for 5-FU without surgery; and 26 days for control. Two animals in the neo-neoadjuvant group were free of tumor when sacrificed at day-165 post-surgically. The results in this study indicate that new treatment strategies for resecting colon cancer liver metastasis should be further explored and the novel regimes introduced in the study of the model could be of great value for designing further clinical trials (Rashidi B, Hoffman RM, unpublished data).

F. Development of patient-tumor SOI models

The first model developed with SOI was for human patient colon cancer [1]. The human patient and human xenograft colon tumors transplanted by SOI resulted in clinically relevant courses such as liver metastasis, lymph node metastasis and peritoneal carcinomatosis (1). The initial "take" rates for human patient colon tumors transplanted by SOI were greater than 80%. In a study of colorectal cancer with the University of California, San Diego (UCSD), Department of Surgery, we have successfully transplanted colon rectal cancer specimens from 16 patients using SOI. In each case, we have been able to passage the tumor to form large cohorts. The tumors have demonstrated liver metastasis,

lymph node metastasis and other clinically-relevant events. Both primary tumors and liver metastasis from patients have been used for SOI (Table 1). In a recent study, we have developed an ultra-metastatic SOI model of human colon cancer with all animals having liver and lymph node metastases by day 10 [62]. Banks of patient tumors which are established in the SOI models are being developed of all the major tumor types (see section G below).

G. Establishment and expansion of SOI tumor models

Patient-derived tumors can be established by SOI with take rates of up to 100% [1,5,62,66–70]. It has been shown to be straightforward to expand an SOI tumor population by serial passage to produce large cohorts of 100 or more SOI animals with the tumor phenotype remaining stable. Established tumors can be serially passaged with nearly 100% efficiency [1,8,62,66–70]. Such expansion allows the SOI models to serve as an important research and development tool. Making large mouse cohorts with identical tumors available is essential for drug discovery and development and has been achieved [1,8,62,66–70].

The SOI technology is effective with a wide variety of patient cancers. We have constructed SOI models of patient cancers of the colon [1,8], lung [4,24,26,27], head and neck (unpublished data), pancreas [5], stomach [4], ovarian [15], liver [37] and breast [22]. Regardless of whether the tumors are passaged subcutaneously or orthotopically, once implanted orthotopically they resemble the donor tissue in detailed morphology, and pattern of growth and metastatic behavior.

The SOI models solve two very major problems in cancer research. Provision of animal models that are more representative of clinical cancer for antitumor and antimetastatic drug discovery and research. The SOI models are also used for producing human primary and metastatic tumor tissue, on demand, with precisely defined characteristics and in large amounts for study of tumor biology, diagnostics development and pharmacogenomics studies.

H. Validation of the SOI models

The SOI tumors have demonstrated a close replication of the original tumor. Apparently the analogous mouse host tissue closely replicates the original patient micro-environment which affects tumor progression and chemosensitivity. For example, an orthotopic model of human small cell lung carcinoma (SCLC) demonstrates sensitivity to cisplatin and resistance to mitomycin C, reflecting the clinical situation [20]. In contrast, the same tumor xenograft implanted subcutaneously responded to mitomycin and not to cisplatin, thus failing to match clinical behavior for SCLC [20]. These data suggest that the orthotopic site is essential to achieve clinically-relevant drug response. Other laboratories have observed similar phenomena indicating the effect of the micro-environnent on drug sensitivity [77].

In order to further understand the role of the host organ in tumor progression, we have transplanted into nude mice histologically-intact human colon cancer tissue on the serosal layers of the stomach (heterotopic site) and the serosal layers of the colon (orthotopic site) [31]. Human colon tumor, Co-3, which is well differentiated, and COL-3-JCK which is poorly differentiated were used for transplantation. After orthotopic transplantation of the human colon tumors on the nude mouse colon, the growing colon tumors resulted in macroscopically extensive invasive local growth in 4 of 10 mice, serosal spreading in 9 of 10 mice, musclaris propria invasion in 1 of 10 mice, submucosal invasion in 3 of 10 mice, mucosal invasion in 3 of 10 mice, lymphatic duct invasion in 4 of 10 mice, regional lymph node metastasis in 4 of 10 mice, and liver metastasis in 1 of 10 mice. In striking contrast, after heterotopic transplantation of the human colon tumor on the nude mouse stomach, a large growing tumor resulted but with only limited invasive growth and without serosal spreading lymphatic duct invasion, or regional lymph node metastasis. It has become clear from these studies that the orthotopic site, in particular the serosal and subserosal transplant surface, is critical to the growth, spread, and invasive and metastatic capability of the implanted colon tumor in nude mice. These studies suggest that the original host organ plays a critical role in tumor progression.

Established human colon and stomach tumors were transplanted by SOI to nude mice and tested for response to 5-FU and mitomycin-C, the standard treatments for these tumors [16,18]. The tumors responded to a dose level that was the mouse equivalent of typical clinical doses. The primary tumors responded as would be expected in the clinic for these agents. The metastases of these tumors were drug-insensitive which replicates the usual clinical situation [16,18]. It was demonstrated that antineoplastic agents can exhibit differential activity against metastases versus primary tumors in SOI models for pancreatic [19], colon [16] and stomach cancer [18]. Importantly,

Table 1. Human patient colon cancer SOI models

Case	Site	Stage	Grade
AC 3438	Colon	T3N0M0	Well diff
AC 3445	Right Colon	Stage II – T3N0M0	Well diff
AC 3488	Sigmoid Colon	Stage IV – T3N1M1	Poorly diff
AC 3508	Sigmoid Colon	Stage IV – T3N1M1	Mod well diff
AC 3518	Sigmoid Colon	Stage III – T3N1M0	Well diff
AC 3521	Cecal Area	Stage III – T2N1M0	Well diff
AC 3528	Polyposis coli	Stage IV – T3N2M1 (liver)	Mod diff
AC 3557	Sigmoid Colon	Stage II – T2N0M0	Welldiff
AC 3603	Transverse Colon	Stage I – TIN0M0	Well diff
AC 3609	Rectal	Stage III – T3N1M0	Mod poor diff
AC 3612	Ascending Colon	Stage II – T3N0M0	Mod diff
AC 3624	Rectal	Stage II – T3N0M0	Well diff
AC 3625	Rectal	Stage III – T3N2M0	Mod diff
AC 3653	Ascending Colon	Stage III –T4N2M0	Well diff

we have demonstrated that very low passage patient colon tumors transplanted by SOI can respond to 5-FU, the standard drug of treatment for this disease (unpublished data).

A correlative clinical trial was carried out to compare the course of stomach tumors in patients and in SOI models after orthotopic transplantation [14]. Of the twenty patient cases whose tumors grew in the nude mice, 6 had clinical peritoneal involvement of their tumor, and of these, 5 resulted in peritoneal metastases in the nude mice. Of the 14 patients without peritoneal involvement whose primary tumors grew locally in the mice, none gave rise to peritoneal involvement in the mice. Of the twenty patient cases, 5 had clinical liver metastases and 15 did not. After SOI of the patient's primary tumors, all 5 primary tumors from the patients with clinical liver metastases gave rise to liver metastases in the nude mice. In contrast, of the 15 primary tumors from patients without liver metastases, only one primary tumor gave rise to liver metastases in the nude mice after SOI. There was a statistical correlation ($p < 0.01$) for both liver metastases and peritoneal involvement between patients and SOI mice. These results indicate that, after surgical orthotopic transplantation of histologically intact gastric cancers from patients to nude mice, the subsequent local and metastatic behavior of the tumor in the mice closely correlated with the course of the tumors in the patients. The histology of both the local and metastatic tumors in the mice closely resembled the original local and metastatic tumors in the patient. These results indicate that the SOI models resemble clinical cancer and correlate with the patient's clinical course and should be useful for drug discovery for both antitumor and antimetastatic agents [14].

I. Bone metastasis in SOI models

1. Breast cancer

The mechanisms of breast cancer metastasizing to bone have been extensively studied [80–82], but remain poorly understood. One of the major impediments is the lack of an accurate animal model [83]. Although human breast cancer cells injected into the mammary fat pad of nude mice can metastasize to the soft organs such as the lung and lymph nodes, spontaneous metastasis of non-selected tumor cell lines to bone has not been reported [84–88]. Bone metastasis thus far has been achieved by injecting breast cancer cells into the left ventricle [89–93] or directly into the bone of nude mice [94]. An orthotopic cell-suspension model of a fgf-transformed MCF-7 human breast cancer cell line demonstrated some bone metastasis [87].

We have developed a spontaneous, highly metastatic nude mice model of human breast cancer, MDA-MB-435, with SOI. Histologically intact MDA-MB-435 tumor tissues were implanted into the mammary fat pads of female nude mice. The results showed extensive metastasis to numerous soft organs and throughout the skeletal system in every transplanted

animal. Orthotopic tumor growth and metastasis occurred throughout the axial skeleton at very high incidence (vertebra 96%, femur 88%, tibia 88%, fibula 64%, humerus 88%, sternum 76%, scapula 40%, skull 24%, rib 44%, pelvis 24% and maxillofacial region 20%) in the SOI animals. Bone metastasis occurred in 25 of 25 transplanted animals. Extensive metastasis also involved numerous visceral organs including lung, lymph node, heart, spleen, diaphragm, adrenal gland, spinal cord, skeletal muscles, parietal pleural membrane, peritoneal cavity, pancreas, liver and kidney. Histologically, the involved bones had obvious osteolytic changes, mimicking clinical bone metastasis in breast cancer. To our knowledge, this is the first report demonstrating extensive spontaneous bone metastasis of human breast cancer from the orthotopic site in nude mice. This clinically accurate model of human estrogen-receptor-negative, advanced breast cancer should be of significant value for the study and development of effective treatment of bone and other metastasis of human breast cancer (An, Z. and Hoffman, R.M., unpublished data).

2. Prostate cancer

We have developed new models of human and animal cancer by transfer of the *Aequorea victoria* jellyfish green fluorescent protein (GFP) gene to tumor cells that enabled visualization of fluorescent tumors and metastases at the microscopic level in fresh viable tissue after transplantation [49,51–53,55,61] (see section K below). We have now developed a fluorescent spontaneous bone metastatic SOI model of human prostate cancer. Fragments of a fluorescent subcutaneously-growing tumor were implanted by SOI in the prostate of a series of nude mice. Subsequent micro-metastases and metastases were visualized by GFP fluorescence throughout the skeleton including the skull, rib, pelvis, femur and tibia. The central nervous system was also involved with tumor, including the brain and spinal cord, as visualized by GFP fluorescence. Systemic organs including the lung, plural membrane, liver, kidney, adrenal gland also had fluorescent metastases. The metastasis pattern in this model accurately reflects the bone and other metastatic sites of human prostate cancer [64]. In previous orthotopic transplant models of human prostate cancer, Stephenson et al. [95], Fu et al. [11], Pettaway et al. [96], Saito et al. [97], Rembrink et al. [98] An et al. [58] and Wang et al. [65] have observed prostate cancer metastasis but only in the lymph nodes and the lung. Thalmann et al. reported a spontaneous bone metastasis model of androgen-independent human prostate cancer LNCaP sublines. The animals developed bone metastasis in 10% and 21.5% of intact and castrated hosts, respectively, after orthotopic injection of cell suspensions [99].

3. Lung cancer

In order to understand the skeletal metastatic pattern of non-small-cell lung cancer, we developed a stable high-expression GFP transductant of human lung cancer cell line H460 (H460-GFP) (see section K below). The GFP-expressing lung cancer was visualized to metastasize widely throughout the skeleton when implanted orthotopically in nude mice. Micrometastases were visualized by GFP fluorescence in the contralateral lung, plural membrane and widely throughout the skeletal system including the skull, vertebra, femur, tibia, pelvis and bone marrow of the femur and tibia. This new metastatic model can play a critical role in the study of the mechanism of skeletal and other metastasis in lung cancer and in screening of therapeutics which prevent or reverse this process [61].

J. Ultrametastatic SOI model of colon cancer

An ultra-high metastatic SOI model of human colon cancer was established from a histologically intact liver metastasis fragment derived from a surgical specimen of a patient with metastatic colon cancer [62]. The stably ultra-metastatic SOI model is termed AC3488UM. 100% of mice transplanted with AC3488UM with SOI to the colon exhibited local growth, regional invasion, and spontaneous metastasis to the liver and lymph nodes. Liver metastases were detected by the tenth day after transplantation in all animals. Half the animals died of metastatic tumor 25 days after transplantation. Histological characteristics of AC3488UM tumor were poorly differentiated adenocarcinoma of colon. Mutant p53 is expressed heterogeneously in the primary tumor and more homogeneously in the liver metastasis suggesting a possible role of p53 in the liver metastasis. The human origin of AC3488UM was confirmed by positive fluorescence staining for *in situ* hybridization of human DNA. The AC3488 human colon tumor model with its ultra-high metastatic capability in each transplanted animal, short latency and a short median survival period is different from any known human colon cancer model and will be an important tool for the study of and development of new therapy for highly metastatic human colon cancer [62].

Future studies will be done to develop SOI models of CNS malignancies and pediatric tumors.

K. Stable expression of the green fluorescent protein (GFP) in cancer cells and tissue to visualize metastasis

The visualization of tumor cell emboli, micrometastases and their progression over real-time during the course of the disease has been difficult in current models of metastasis. Previous studies used transfection of tumor cells with the *Escherichia coli* beta-galactosidase (lacZ) gene to detect micrometastases [100,101]. However, detection of lacZ requires extensive histological preparation, and therefore it is impossible to detect and visualize tumor cells in viable fresh tissue or the live animal at the microscopic level. The visualization of tumor invasion and micrometastasis formation in viable fresh tissue or the live animal is necessary for a critical understanding of tumor progression and its control.

To enhance the resolution of the visualization of micrometastases in fresh tissue, we have utilized the green fluorescent protein (GFP) gene, cloned from the bioluminescent jellyfish *Aequorea victoria* [102–116]. GFP has demonstrated its potential for use as a marker for gene expression in a variety of cell types [103,104]. The GFP cDNA encodes a 283 amino acid polypeptide with molecular weight of 27 kD [105,106]. The monomeric GFP requires no other *Aequorea* proteins, substrates, or cofactors to fluoresce [107]. Recently, GFP gene gain-of-function mutants have been generated by various techniques [108,110]. For example, the GFP-S65T clone has the serine-65 codon substituted with a threonine codon which results in a single excitation peak at 490 nm [108,109]. Moreover, to develop higher expression in human and other mammalian cells, a humanized hGFP-S65T clone was isolated [111]. The much brighter fluorescence in the mutant clones allows for easy detection of GFP expression in transfected cells.

We have isolated 50 GFP transfectants of human and animal cancer cells that are stable *in vitro* and *in vivo* [49,51,52]. The transfectants are highly fluorescent *in vivo* in tumors formed from the cells. Using these fluorescent transfectants, orthotopic-transplant animal models [26,61,64,112] were utilized for visualizing the metastatic processes in fresh tissue down to the single cell level that heretofore was not possible.

L. GFP-expressing macro- and micrometastases of CHO-K1 in nude mice in SOI models

Nude mice were implanted with 1-mm^3 cubes of GFP-CHO-K1 tumor into the ovary and were sacrificed at four weeks [49]. All mice had tumors in the ovaries. The tumor had also seeded throughout the peritoneal cavity, including the colon, cecum, small intestine, spleen, and peritoneal wall. The primary tumor and peritoneal metastases were strongly fluorescent. Numerous micrometastases were detected by fluorescence on the lungs of all mice. Multiple micrometastases were also detected by fluorescence on the liver, kidney, contralateral ovary, adrenal gland, para-aortic lymph node, and pleural membrane at the single-cell level. Single-cell micrometastases could not be detected by standard histological techniques. Even multiple-cell small colonies were difficult to detect by hematoxylin and eosin staining, but they could be detected and visualized clearly by GFP fluorescence. Some colonies were observed under confocal microscopy. As these colonies developed, the density of tumor cells was markedly decreased in the center of the colonies.

M. Patterns of lung tumor metastases of human lung tumors visualized by GFP expression in SOI models

Primary tumor grew in the operated left lung in all mice after SOI of human lung tumor GFP-ANIP-973. GFP expression allowed visualization of the advancing margin of the tumor spreading in the ipsilateral lung. All animals explored had evidence of chest wall invasion and local and regional spread. Metastatic contralateral tumors involved the mediastinum, contralateral pleural cavity, the contralateral visceral pleura. While the ipsilateral tumor had a continuous and advancing margin, the contralateral tumor seems to have been formed by multiple seeding events. These observations were made possible by GFP fluorescence of the fresh tumor tissue [51,52]. Contralateral hilar lymph nodes were also involved as well as cervical lymph nodes shown by GFP expression. A cervical lymph node metastasis was brightly visualized by GFP in fresh tissue [51,52]. When non-GFP-transfected ANIP-973 was compared with GFlP-transformed ANIP-973 for metastatic capability similar results were seen [51].

Nude mice were implanted in the left lung by SOI with 1-mm^3 cubes of human H460-GFP tumor tissue derived from the H460-GFP subcutaneous tumor [61]. The implanted mice were sacrificed at three to

four weeks at the time of significant decline in performance status. All mice had tumors in the left lung. All tumors (8/8) metastasized to the contralateral lung, and chest wall. Seven of eight tumors metastasized to the skeletal system. It was determined that the vertebrae were the most involved skeletal site of metastasis, since 7 of 8 mice had vertebral metastasis. Three of seven mice had skull metastases visualized by GFP. Metastasis could also be visualized in the tibia and femur marrow by GFP fluorescence. The tumor lodged in the bone marrow and seemed to begin to involve the bone as well. All of the experimental animals were found with contralateral lung metastases [61]. Extensive and widespread skeletal metastasis, visualized by GFP expression, were found in approximately 90% of the animals explored. Thus, the H460-GFP SOI model revealed the extensive skeletal metastasizing potential of lung cancer. Such a high incidence of skeletal metastasis could not have been previously visualized before the development of the GFP-SOI model described here which provided the necessary tools.

N. Bone and visceral metastasis of human prostate cancer PC-3 visualized by GFP in SOI models

Five of five mice developed strongly fluorescent orthotopic tumors. Three of five tumors metastasized to the skeletal system. The skeletal metastasis included the skull, rib, pelvis, femur, and tibia. All the tumors metastasized to the lung, pleural membrane and kidney. Four of five tumors metastasized to liver and two of five tumors metastasized to the adrenal gland. In two mice, cancer cells or small colonies were seen in the brain and in one mouse a few cells were in the spinal cord by GFP fluorescence [64].

O. In vivo *videomicroscopy to follow steps of metastasis*

We took advantage of stable GFP-transfected cells for monitoring and quantifying sequential steps in the metastatic process [113]. Using GFP-CHO-K1, the visualization of sequential steps in metastasis within mouse liver, from initial arrest of cells in the microvasculature to the growth and angiogenesis of metastases were quantified by intravital videomicroscopy. Individual, non-dividing cells, as well as micro- and macrometastases could clearly be detected and quantified, as could fine cellular details such as pseudopodial projections, even after extended periods of *in vivo* growth. The GFP-fluorescent tumor cells had preferential growth and survival of micrometastases near the liver surface. Furthermore, we observed a small population of single cells that persisted over the 11-day observation period, which may represent dormant cells with potential for subsequent proliferation. This study demonstrated the advantages of GFP-expressing cells, coupled with real-time high resolution videomicroscopy, for long-term *in vivo* studies to visualize and quantify sequential steps of the metastatic process.

GFP-transfected murine mammary adenocarcinoma cells inoculated into various sites of the rat were visualized colonizing various organs by video microscopy [114].

P. Transgenic mouse models of cancer

Examples of transgenic mouse cancer models are outlined below for comparison with SOI models:

1. Breast cancer

Stewart et al. [115] and Sinn et al. [116] developed transgenic mice in which expression of the c-*myc* or v-Ha-*ras* oncogenes or both were targeted to mammary tissue using the MMTV (mouse mammary tumor virus) long terminal repeat promoter. Both lines of mice, MMTV-myc [115,116] and MMTV-ras [116], were found to have mammary tumors after several months of life. In lines with both oncogenes, tumors developed more rapidly than either of the single transgenic lines [116]. In one strain, all surviving F1 female progeny that inherited the MTV/*myc* fusion gene developed breast tumors at 5 to 6 months of age during their second or third pregnancies [115]. The tumors in the double transgenics arose in a stochastic fashion, as solitary adenocarcinomas or as monoclonal B cell lymphomas [116].

Mice expressing the polyomavirus middle T-antigen (MTAg) under the control of the MMTV promoter/enhancer (MMTV-MTAg mice) had synchronous multifocal mammary adenocarcinoma with a short latency period and a high rate of metastasis to lung. Not all tumors in MMTV-MTAg mice are uniform or synchronous. All mice with established primary mammary tumors did not have metastatic disease [117,118].

MMTV-*neu* transgenic mice overexpress *neu* in the mammary epithelium and develop focal, frequently metastatic mammary adenocarcinoma after a relatively long latency period [119].

A transgenic mouse strain was constructed with the mammary tumor virus LTR/c-*myc* fusion gene. The glucocorticoid inducible c-*myc* transgene led to an

increased incidence of breast, testicular, and lymphocytic (B-cell and T-cell), and mast cell tumors [120].

2. Prostate cancer

A recombinant probasin (PB)-SV40 Tag (T antigen) transgenic mouse was developed [121,122]. These transgenic animals were termed TRAMP (transgenic adenocarcinoma mouse prostate) [121,122]. In TRAMP mice, expression of the PB-Tag transgene is restricted to the dorsolateral lobes of the prostate. TRAMP mice have high-grade PIN (prostatic intraepithelial neoplasia) and/or well-differentiated prostate cancer by the age of 10–12 weeks [123]. TRAMP mice spontaneously develop invasive primary tumors that routinely metastasize to the lymph nodes and lungs and less frequently metastasize to the spinal column, kidneys, and adrenal glands [122]. Hind limb paraplegia was observed in a single TRAMP mouse at the age of 22 weeks. Histological examination of decalcified sections of the spine at the level of the thoracolumbar vertebrae demonstrated that the spinal canal was filled with metastatic tumor. The tumor appeared to have destroyed the spinal cord through pressure atrophy rather than by invasion and destruction of the adjacent vertebral bone as typically seen with osteolytic metastatic tumors [122]. Lymph node metastases were found in 31% (5 of 16) of TRAMP mice between 18 and 24 weeks of age. Pulmonary metastases were found in 4 of 11 (36%) by 24 weeks. A metastasis in the kidney has been found in one mouse at 12 weeks. Two metastases to the adrenal gland were found [122]. At 30–36 weeks of age, 100% of TRAMP animals have primary tumors and metastatic disease [122,123].

3. Colon cancer

The Smad3 gene was inactivated in mice by homologous recombination. Homozygous mutants were viable and spontaneously formed colorectal adenocarcinomas [124]. Between 4 and 6 months of age, the Smad3 mutant mice became moribund with the colorectal adenocarcinomas. The colorectal cancers penetrated through all layers of the intestinal wall and metastasized to lymph nodes [124].

4. p53 knockouts

Homozygote p53-deficient mice, and normal littermates (with wild-type p53 genes) were monitored for spontaneous neoplasms [125]. Wild-type mice (95 animals) by the age of 9 months did not develop tumors. By 9 months, only 2 of 96 heterozygote animals developed tumors. One heterozygote mouse developed an embryonal carcinoma of the testis at 5 months and another developed a malignant lymphoma at the age of 9 months [125]. Of 35 homozygote animals, 26 (74%) developed neoplasms by 6 months of age. Some tumors appeared before 10 weeks of age, and tumor occurrence increased rapidly between 15 and 25 weeks of age [125]. Multiple primary neoplasms of different origin were observed in 9 of the 26 homozygote mice with tumors. Malignant lymphomas were found in 20 of 26 animals. Sarcomas also occurred with some frequency. There were seven hemangiosarcomas, three undifferentiated sarcomas, and one osteosarcoma. Only one female mouse developed a mammary adenocarcinoma [125].

It can be clearly seen that the transgenic mouse models of breast, prostate and colon cancer do not reflect human clinical cancer as do the SOI models. For example, the transgenic breast cancer models to not metastasize to the bone; the prostate cancer transgenic model metastasized to the bone in only one reported animal; the colon cancer transgenic model did not metastasize to the liver, and in the p53 knockout models only one animal had breast cancer. The SOI models thus offer unique and critically important features for antitumor and antimetastatic drug discovery.

Materials and methods

A. General construction of models

1. Mice

Four-to-six-week old outbred nu/nu mice of both sexes are used for the orthotopic transplantation. All the mice are maintained in a pathogen-free environment. Cages, bedding, food and water are autoclaved and changed regularly. All the mice are maintained in a daily cycle of 12 hour period of light and darkness. Bethaprim Pediatric Suspension (containing sulfamethoxazole and trimethoprim) is added to the drinking water. Mice are periodically sent to the University of Missouri to test for pathogens. All animal studies were conducted in accordance with the principles and procedures outlined in the National Institutes of Health Guide for the Care and Use of Laboratory Animals under assurance number A3873-1.

2. Specimens

Fresh surgical specimens are kept in Earle's MEM at 4°C and obtained as soon as possible from hospitals.

Transplantation should take place within 24 hours of surgical excision. Before transplantation, each specimen is inspected, and all necrotic and suspected necrotic tumor tissue is removed. To take into account tumor heterogeneity, each specimen is equally divided into 5 parts, separated and each part is subsequently cut into small pieces of about 1 mm^3 size. Tumor pieces for each transplantation are taken from 5 parts of each specimen equally. In our experience, a typical colon tumor specimen of 1–2 grams provides sufficient material for initial surgical orthotopic implantation of more than 20 mice. Additional SOI models of this same tumor can subsequently be generated by a single passage using SOI. It should be noted that patient tumors are routinely passaged orthotopically to produce large cohorts. One hundred mice or more can be readily transplanted in the first passage which are more than sufficient for treatment studies.

B. Examples of surgical orthotopic implantation (SOI)

1. Colon cancer

Colonic transplantation For transplantation, nude mice are anesthetized, and the abdomen is sterilized with iodine and alcohol swabs. A small midline incision is made and the colorectal part of the intestine is exteriorized. Serosa of the site where tumor pieces are to be implanted is removed. Eight pieces of 1-mm^3 size tumor are implanted on the top of the animal intestine. An 8-0 surgical suture is used to penetrate these small tumor pieces and attach them on the wall of the intestine. The intestine is returned to the abdominal cavity, and the abdominal wall is closed with 7-0 surgical sutures (Figure 1). Animals are kept in a sterile environment. Tumors of all stages and grades can be utilized [1].

Intrahepatic transplantation An incision is made through the left upper abdominal pararectal line and peritoneum. The left lobe of the liver is carefully exposed and the liver is cut about 3 mm with scissors. Two to three tumor pieces of 1–2 mm^3 size are put on the nude mouse liver and attached immediately with double sutures using 8-0 nylon with an atraumatic needle. After confirmation that no bleeding is occurring, the liver is then returned to the peritoneal cavity. The abdomen and skin are then closed with 6-0 back silk sutures [30].

2. Prostate cancer

Tumor fragments are prepared as for colon and breast tumors. Two tumor fragments (1 mm^3) are implanted by SOI in the dorsolateral lobe of the prostate. After proper exposure of the bladder and prostate following a lower midline abdominal incision, the capsule of the prostate is opened and the two tumor fragments are inserted into the capsule. The capsule is then closed with an 8-0 surgical suture. The incision in the abdominal wall is closed with a 6-0 surgical suture in one layer [11,64,65].

3. Lung cancer

The mice are anesthetized by isoflurane inhalation. The animals are put in a position of right lateral decubitus, with four limbs restained. A 0.8 cm transverse incision of skin is made in the left chest wall. Chest muscles are separated by sharp dissection and costal and intercostal muscles are exposed. A 0.4–0.5 cm intercostal incision between the third and fourth rib on the chest wall is made and the chest wall is opened. The left lung is taken up with a forceps and tumor fragments are sewn promptly into the upper lung with one suture. The lung is then returned into the chest cavity. The incision in the chest wall is closed by a 6-0 surgical suture. The closed condition of the chest wall is examined immediately and if a leak exists, it is closed by additional sutures. After closing the chest wall, an intrathoracic puncture is made by using a 3-ml syringe and 25G $\frac{1}{2}$ needle to withdraw the remaining air in the chest cavity. After the withdrawal of air, a completely inflated lung can be seen through the thin chest wall of the mouse. Then the skin and chest muscle are closed with a 6-0 surgical suture in one layer [61] (Figure 2).

C. Cohorts of transplanted animals for treatment

Cohorts of over 100 SOI models have been constructed from many SOI models. The “take rate” for transplantation after the first passage is generally 100%. Cohorts of 100 mice per case can be easily constructed [62].

D. Determination and characterization of xenografted tumors

Complete autopsy with histological examination is performed on all mice at time of death. All of the major organs are examined carefully and routinely sampled, along with any tissues showing gross abnormalities.

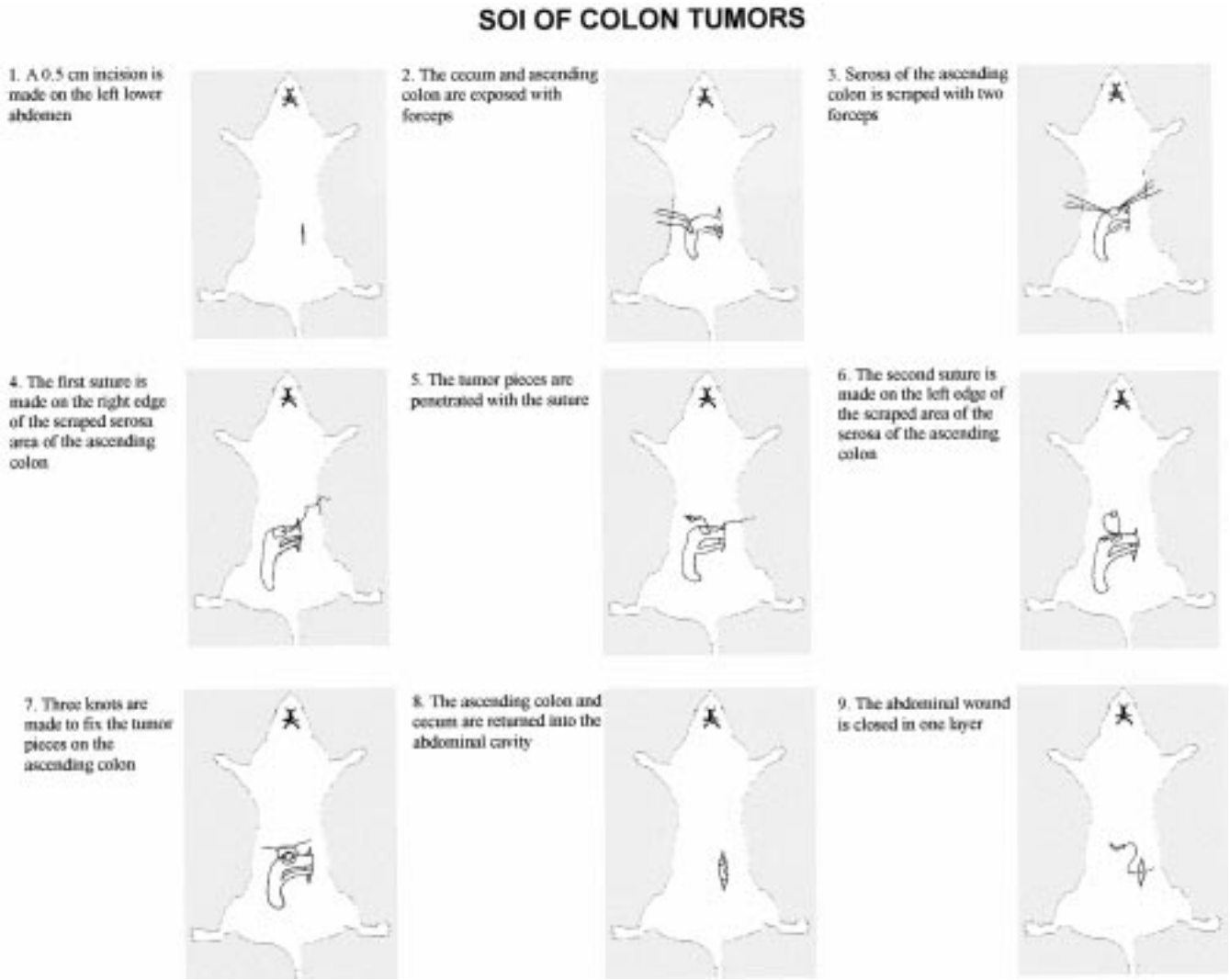
SOI OF COLON TUMORS
1. A 0.5 cm incision is made on the left lower abdomen
2. The cecum and ascending colon are exposed with forceps
3. Serosa of the ascending colon is scraped with two forceps
4. The first suture is made on the right edge of the scraped serosa area of the ascending colon
5. The tumor pieces are penetrated with the suture
6. The second suture is made on the left edge of the scraped area of the serosa of the ascending colon
7. Three knots are made to fix the tumor pieces on the ascending colon
8. The ascending colon and cecum are returned into the abdominal cavity
9. The abdominal wound is closed in one layer

Figure 1.

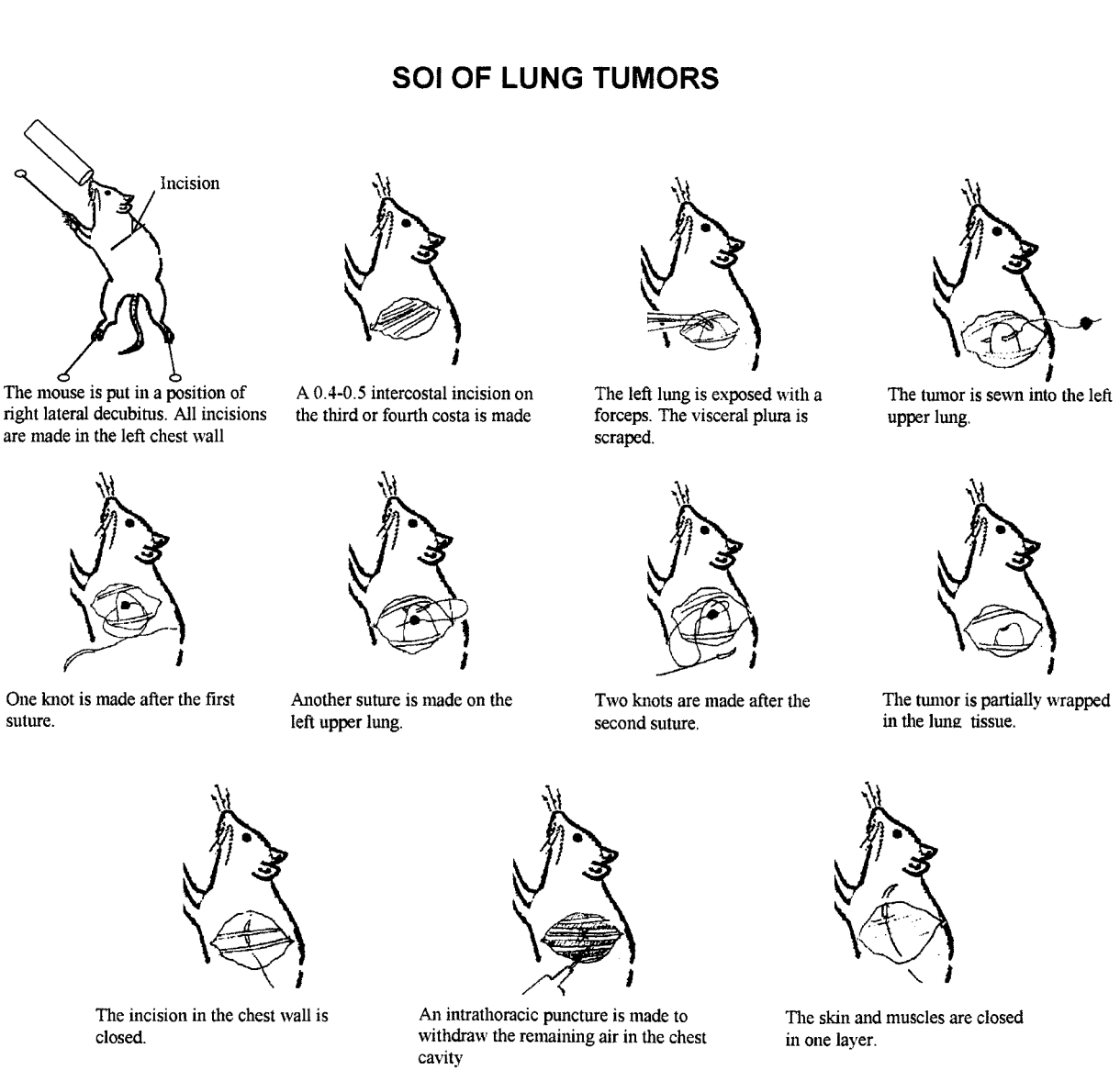
SOI OF LUNG TUMORS
Incision
The mouse is put in a position of right lateral decubitus. All incisions are made in the left chest wall
A 0.4-0.5 intercostal incision on the third or fourth costa is made
The left lung is exposed with a forceps. The visceral plura is scraped.
The tumor is sewn into the left upper lung.
One knot is made after the first suture.
Another suture is made on the left upper lung.
Two knots are made after the second suture.
The tumor is partially wrapped in the lung tissue.
The incision in the chest wall is closed.
An intrathoracic puncture is made to withdraw the remaining air in the chest cavity
The skin and muscles are closed in one layer.

Figure 2.

E. Evaluation of growth and metastasis of orthotopically transplanted tumors

The mice are autopsied and analyzed histologically for the presence of local growth and metastases upon sacrifice after they become moribund. Mice are killed if they develop signs of distress. For example, in the colon tumor models the distress symptoms include a decline in performance status and weight loss due to cachexia or drug treatment. At autopsy, the colon and all peritoneal organs, lymph nodes, liver and lungs are resected and processed for routine histological examination for tumors after careful microscopic examination. Metastases are considered to have occurred if at least one microscopic metastatic lesion is found in any of the animals. The growth of locally growing tumors is determined by caliper measurement of the locally growing tumor which is possible for colon tumors, since the body wall is so thin, and by weighing the tumors that are removed at autopsy. Caliper measurements of the primary tumor can also allow determination of tumor regression. The primary tumor is weighed at autopsy.

1. Isolation of stable high expression GFP tumor cells

The GFP expression vector RetroXpress vector pLEIN is purchased from CLONTECH Laboratories, Inc. (Palo Alto, CA). The pLEIN vector expresses enhanced green fluorescent protein (EGFP) and the neomycin resistance gene on the same bicistronic message which contains an IRES site [61,64]. For GFP gene transduction, 20%-confluent cancer cells are incubated with a 1:1 precipitated mixture of retroviral supernatants of PT67 packaging cells and RPMI 1640 (GIBCO) containing 10% fetal bovine serum (FBS) (Gemini Bio-products, Calabasas, CA) for 72 hours. Fresh medium is replenished at this time. Cells are harvested by trypsin/EDTA 72 hours post-infection, and subcultured at a ratio of 1:15 into selective medium which contains 200 μg/ml of G418. The level of geneticin (G418) (Life Technologies, Grand Island, NY) is increased to 800–1000 μg/ml gradually. Clones expressing GFP are isolated with cloning cylinders (Bel-Art Products, Pequannock, NJ) by trypsin/EDTA and are amplified and transferred by conventional culture methods [61,64].

2. Analysis of GFP-expressing metastases

Mice are sacrificed when their performance status begins to decline and the systemic organs are removed. The orthotopic primary tumor and all major organs as well as the whole skeleton are explored. The fresh samples are sliced at approximately 1 mm thickness and observed directly under fluorescence microscopy. The samples are also processed for histological examination for fluorescence in frozen sections. The slides are then rinsed with phosphate-buffered saline (PBS) and then fixed for 10 minutes at 4°C in 2% formaldehyde plus 0.2% gluteraldehyde in PBS. The slides are washed with PBS and stained with hematoxylin and eosin using standard techniques.

3. Microscopy

Light and fluorescence microscopy are carried out using a Nikon microscope equipped with a Xenon lamp power supply. A Leica stereo fluorescence microscope model LZ12 equipped with a mercury lamp power supply are also used. Both microscopes have a GFP filter set (Chroma Technology, Brattleboro, VT). An MRC-600 confocal imaging system (Bio-Rad) mounted on a Nikon microscope with an argon laser is also used. Photomicrographs are processed for brightness and contrast with Image Pro Plus, Version 3.0, software (Media Cybernetics, Silver Springs, MD).

References

1. Fu X, Besterman JM, Monosov A, Hoffman RM: Models of human metastatic colon cancer in nude mice orthotopically constructed by using histologically-intact patient specimens. Proc Natl Acad Sci USA 88: 9345–9349, 1991
2. Fu X, Theodorescu D, Kerbel RS, Hoffman RM: Extensive multi-organ metastasis following orthotopic on plantation of histologically-intact human bladder carcinoma tissue in nude mice. Int J Cancer 49: 938–939, 1991
3. Fu X, Hoffman RM: Human RT-4 bladder carcinoma is highly metastatic in nude mice and comparable to ras-H-transformed RT-4 when orthotopically onplanted as histologically-intact tissue. Int J Cancer 51: 989–991, 1992
4. Wang X, Fu X, Hoffman RM: A new patient-like metastatic model of human lung cancer constructed orthotopically with intact tissue via thoracotomy in immunodeficient mice. Int J Cancer 51: 992-995, 1992
5. Fu X, Guadagni F, Hoffman RM: A metastatic nude-mouse model of human pancreatic cancer constructed orthotopically from histologically-intact patient specimens. Proc Natl Acad Sci USA 89: 5645–5649, 1992
6. Hoffman RM: Patient-like models of human cancer in mice. Current Perspectives on Molecular & Cellular Oncology 1(B): 311–326, 1992
7. Kuo, T-H, Kubota T, Watanabe M, Furukawa T, Kase S, Tanino H, Nishibori K, Saikawa Y, Teramoto T, Ishibiki K, Kitajima M, Hoffman RM: Orthotopic reconstitution of human small-cell lung carcinoma after intravenous transplantation in SCID mice. Anticancer Res 12: 1407–1410, 1992
8. Fu X, Herrera H, Kubota T, Hoffman RM: Extensive liver metastasis from human colon cancer in nude and scid mice

after orthotopic onplantation of histologically-intact human colon carcinoma tissue. Anticancer Res 12: 1395–1398, 1992
9. Wang X, Fu X, Hoffman RM: A patient-like metastasizing model of human lung adenocarcinoma constructed via thoracotomy in nude mice. Anticancer Res 12: 1399–1402, 1992
10. Wang X, Fu X, Kubota T, Hoffman RM: A new patient-like metastatic model of human small-cell lung cancer constructed orthotopically with intact tissue via thoracotomy in immunodeficient mice. Anticancer Res 12: 1403–1406, 1992
11. Fu X, Herrera H, Hoffman RM: Orthotopic growth and metastasis of human prostate carcinoma in nude mice after transplantation in nude mice. Int J Cancer 52: 987–990, 1992
12. Hoffman RM: Histoculture and the immunodeficient mouse come to the cancer clinic: rational approaches to individualizing cancer therapy and new drug evaluation review). Int J Oncol 1: 467–474, 1992
13. Furukawa T, Fu X, Kubota T, Watanabe M, Kitajima M, Hoffman RM: Nude mouse metastatic models of human stomach cancer constructed using orthotopic implantation of histologically-intact tissue. Cancer Research 53: 1204–1208, 1993
14. Furukawa T, Kubota T, Watanabe M, Kitajima M, Fu X, Hoffman RM: Orthotopic transplantation of histologically-intact clinical specimens of stomach cancer to nude mice: Correlation of metastatic sites in mouse and human. Int J Cancer 53: 608–612, 1993
15. Fu X, Hoffman RM: Human ovarian carcinoma metastatic models constructed in nude mice by orthotopic transplantation of histologically-intact patient specimens. Anticancer Res 13: 283–286, 1993
16. Furukawa T, Kubota T, Watanabe M, Kuo PH, Kase S, Saikawa Y, Tanino H, Teramoto T, Ishibiki K, Kitajima M, Hoffman RM: Immunochemotherapy prevents human colon cancer metastasis after orthotopic onplantation of histologically-intact tumor tissue in nude mice. Anticancer Res 13: 287–291, 1993
17. Kuo T-H, Kubota T, Watanabe M, Fujita S, Furukawa T, Teramoto T, Ishibiki K, Kitajima M, Hoffman RM: Early resection of primary orthotopically-growing human colon tumor in nude mouse prevents liver metastasis: Further evidence for patient-like hematogenous metastatic route. Anticancer Res 13: 293–298, 1993
18. Furukawa T, Kubota T, Watanabe M, Kitajima M, Hoffman RM: Differential chemosensitivity of local and metastatic human stomach cancer after orthotopic transplantation of histologically-intact tumor tissue in nude mice. Int J Cancer 54: 397–401, 1993
19. Furukawa T, Kubota T, Watanabe M, Kitajima M, Hoffman RM: A novel "patient-like" treatment model of human pancreatic cancer constructed using orthotopic transplantation of histologically-intact human tumor-tissue in nude mice. Cancer Res 53: 3070–3072, 1993
20. Kuo T-H, Kubota T, Watanabe M, Furukawa T, Kase S, Tanino H, Nishibori H, Saikawa Y, Ishibiki K, Kitajima M, Hoffman RM: Site-specific chemosensitivity of human small-cell lung carcinoma growing orthotopically compared to subcutaneously in SCID mice: The importance of orthotopic models to obtain relevant drug evaluation data. Anticancer Res 13: 627–630, 1993
21. Furukawa T, Kubota T, Watanabe M, Kuo T-H, Nishibori H, Kase S, Saikawa Y, Tanino H, Teramoto T, Ishibiki K, Kitajima M: A metastatic model of human colon cancer constructed using cecal implantation of cancer tissue in nude mice. Jpn J Surg 23: 420–423, 1993
22. Fu X, Le P, Hoffman RM: A metastatic orthotopic transplant nude-mouse model of human patient breast cancer. Anticancer Res 13: 901–904, 1993
23. Astoul P, Colt HG, Wang X, Hoffman RM: Metastatic human pleural ovarian cancer model constructed by orthotopic implantation of fresh histologically-intact patient carcinoma in nude mice. Anticancer Res 13: 1999–2002, 1993
24. Astoul P, Wang X, Hoffman RM: "Patient-Like" nude mouse models of human lung and pleural cancer (Review). Int J Oncology 3: 713–718, 1993
25. Kubota T, Inoue S, Furukawa T, Ishibiki K, Kitajima M, Kawamura E, Hoffman RM: Similarity of Serum – Tumor Pharmacokinetics of Antitumor Agents in Man and Nude Mice. Anticancer Research 13: 1481–1484, 1993
26. Astoul P, Colt HG, Wang X, Hoffman RM: A "patient-like" nude mouse model of parietal pleural human lung adenocarcinoma. Anticancer Res 14: 85–92, 1994
27. Astoul P, Colt HG, Wang X, Boutin C, Hoffman RM: A "patient-like" nude mouse metastatic model of advanced human pleural cancer. J Cell Biochem 56: 9–15, 1994
28. Wang X, Fu X, Brown PD, Crimmin MJ, Hoffman RM: Matrix metalloproteinase inhibitor BB-94 (Batimastat) inhibits human colon tumor growth and spread in a patient-like orthotopic model in nude mice. Cancer Res 54: 4726–4728, 1994
29. Hoffman RM: Orthotopic is orthodox: why are orthotopic-transplant metastatic models different from all other models? J Cell Biochem 56: 1–4, 1994
30. Togo S, Shimada H, Kubota T, Moossa AR, Hoffman RM: Seed to soil is a return trip in metastasis. Anticancer Res 15: 791–794, 1995
31. Togo S, Shimada H, Kubota T, Moossa AR, Hoffman RM: Host organ specifically determines cancer progression. Cancer Res 55: 681–684, 1995
32. Kuo T-H, Kubota T, Watanabe M, Furukawa T, Teramoto T, Ishibiki K, Kitajimi M, Moossa AR, Penman S, Hoffman RM: Liver colonization competence governs colon cancer metastasis. Proc Natl Acad Sci USA 92: 12085–12089, 1995
33. Togo S, Wang X, Shimada H, Moossa AR, Hoffman RM: Cancer seed and soil can be highly selective: Human-patient colon tumor lung metastasis grows in nude mouse lung but not colon or subcutis. Anticancer Res 15: 795–798, 1995
34. Dutton G: AntiCancer Inc. scientists identify a key governing step in the metastasis of cancer. Genetic Engineering News 16: 1, January 15, 1996
35. Holzman D: Of mice and metastasis: a new for-profit model emerges J Natl Cancer Inst 88: 396–397, 1996
36. Leff DN: MetaMouse models colon cancer metastasis with clinical potential. BioWorld Today 7, 1 (January 8), 1996
37. Sun FX, Tang ZY, Liu KD, Ye SL, Xue Q, Gao DM, Ma ZC: Establishment of a metastatic model of human hepatocellular carcinoma in nude mice via orthotopic implantation of histologically intact tissues. Int J Cancer 66: 239–243, 1996
38. An Z, Wang X, Kubota T, Moossa AR, Hoffman RM: A clinical nude mouse metastatic model for highly malignant human pancreatic cancer. Anticancer Res 16: 627–632, 1996
39. Riordan T: A technique is said to ease attachment of tumors to mice, making them "little cancer patients". New York Times, "Patents" Column, March 4, 1996
40. Murray G, Duncan M, O'Neil P, Melvin W, Fothergill J: Matrix metalloproteinase-1 is associated with poor prognosis in colorectal cancer. Nature Med 2: 461–462, 1996

41. Hoffman RM: Fertile seed and rich soil: development of patient-like models of human cancer by surgical orthotopic implantation of intact tissue. Update Series: Comprehensive Textbook of Oncology 3: 1–10, Schimpff, S.C, et al, eds. Williams & Williams, Baltimore, 1996
42. Sun F-X, Tang Z-Y, Liu K-D, Xue Q, Gao D-M, Yu Y-Q, Zhou X-D, Ma Z-C: Metastatic models of human liver cancer in nude mice orthotopically constructed by using histologically intact patient specimens. J Cancer Res Clin Oncol 122: 397-402, 1996
43. Astoul P, Wang X, Colt HG, Boutin C, Hoffman RM: A patient-like human malignant pleural mesothelioma nude-mouse model. Oncology Reports 3: 483–487, 1996
44. Colt HG, Astoul P, Wang X, Yi ES, Boutin C, Hoffman RM: Clinical course of human epithelial-type malignant pleural mesothelioma replicated in an orthotopic-transplant nude mouse model. Anticancer Res 16: 633–640, 1996
45. An Z, Wang X, Astoul P, Danays T, Hoffman RM: Interferon gamma is highly effective against orthotopically-implanted human pleural adenocarcinoma in nude mice. Anticancer Res 16: 2545–2551, 1996
46. Olbina G, Cieslak D, Ruzdijic S, Esler C, An Z, Wang X, Hoffman RM, Seifert W, Pietrzkowski Z: Reversible inhibition of IL-8 receptor B mRNA expression and proliferation in non-small cell lung cancer by antisense oligonucleotides. Anticancer Res 16: 3525–3530, 1996
47. An Z, Wang X, Willmott N, Chander SK, Tickle S, Docherty AJP, Mountain A, Millican AT, Morphy R, Porter JR, Epemolu RO, Kubota T, Moossa AR, Hoffman RM: Conversion of highly malignant colon cancer from an aggressive to a controlled disease by oral administration of a metalloproteinase inhibitor. Clin Exp Metastasis 15: 184–195, 1997
48. Hoffman RM: Fertile seed and rich soil: The development of clinically relevant models of human cancer by surgical orthotopic implantation of intact tissue. In: Teicher B (ed) Anticancer Drug Development Guide: Preclinical Screening Clinical Trials, and Approval. Totowa, NJ: Humana Press Inc., 127–144, 1997
49. Chishima T, Miyagi Y, Wang X, Yamaoka H, Shimada H, Moossa AR, Hoffman RM: Cancer invasion and micrometastasis visualized in live tissue by green fluorescent protein expression. Cancer Res 57: 2042–2047, 1997
50. Inada T, Ichikawa A, Kubota T, Ogata Y, Moossa AR, Hoffman RM: 5-FU-induced apoptosis correlates with efficacy against human gastric and colon cancer xenografts in nude mice. Anticancer Res 17: 1965–1972, 1997
51. Chishima T, Miyagi Y, Wang X, Baranov E, Tan Y, Shimada H, Moossa AR, Hoffman RM: Metastatic patterns of lung cancer visualized live and in process by green fluorescent protein expression. Clin Exp Metastasis 15: 547–552, 1997
52. Chishima T, Miyagi Y, Wang X, Tan Y, Shimada H, Moossa AR, Hoffman RM: Visualization of the metastatic process by green fluorescent protein expression. Anticancer Res 17: 2377–2384, 1997
53. Chishima T, Yang M, Miyagi Y, Li L, Tan Y, Baranov E, Shimada H, Moossa AR, Penman S, Hoffman RM: Governing step of metastasis visualized *in vitro*. Proc Natl Acad Sci USA 94: 11573–11576, 1997
54. Tomikawa M, Kubota T, Matsuzaki SW, Takahasi S, Kitajima M, Moossa AR, Hoffman RM: Mitomycin C and cisplatin increase survival in a human pancreatic cancer metastatic model. Anticancer Res 17: 3623–3626, 1997
55. Chishima T, Miyagi Y, Li L, Tan Y, Baranov E, Yang M, Shimada H, Moossa AR, Hoffman RM: The use of histoculture and green fluorescent protein to visualize tumor cell host interaction. In Vitro Cell Dev Biol 33: 745–747, 1997
56. Chang S-G, Kim JI, Jung J-C, Rho Y-S, Lee K-T, An Z, Wang X, Hoffman RM: Antimetastatic activity of the new platinum analog {Pt(cis-dach)(DPPE)·2NO_3} in a metastatic model of human bladder cancer. Anticancer Res 17: 3239–3242, 1997
57. Dev SB, Nanda GS, An Z, Wang X, Hoffman RM, Hofmann GA: Effective electroporation therapy of human pancreatic tumors implanted in nude mice. Drug Delivery 4: 293–299, 1997
58. An Z, Wang X, Geller J, Moossa AR, Hoffman RM: Surgical orthotopic implantation allows high lung and lymph node metastatic expression of human prostate carcinoma cell line PC-3 in nude mice. Prostate 34: 169–174, 1998
59. Nanda GS, Sun FX, Hofmann GA, Hoffman RM, Dev SB: Electroporation therapy of human larynx tumors HEp-2 implanted in nude mice. Anticancer Res 18: 999–1004, 1998
60. Nanda GS, Sun FX, Hofmann GA, Hoffman RM, Dev SB: Electroporation enhances therapeutic efficacy of anticancer drugs: Treatment of human pancreatic tumor in animal model. Anticancer Res 18: 1361–1366, 1998
61. Yang M, Hasegawa S, Jiang P, Wang X, Tan Y, Chishima T, Shimada H, Moossa AR, Hoffman RM: Widespread skeletal metastatic potential of human lung cancer revealed by green fluorescent protein expression. Cancer Res 58: 4217–4221, 1998
62. Sun F-X, Sasson AR, Gamagami R, Jiang P, Moossa AR, Hoffman RH: An ultra-metastatic model of human colon cancer in nude mice. Clin Exp Metastasis 17(1): 41–48, 1999
63. Kiguchi K, Kubota T, Aoki D, Udagawa Y, Tamanouchi S, Saga M, Amemiya A, Sun F-X, Nozawa S, Moossa AR, Hoffman RM: A patient-like orthotopic implantation nude mouse model of highly metastatic human ovarian cancer. Clin Exp Metastasis 16: 75 1–756, 1999
64. Yang M, Jiang P, Sun FX, Hasegawa S, Baranov E, Chishima T, Shimada H, Moossa AR, Hoffman RM: A fluorescent orthotopic bone metastasis model of human prostate cancer. Cancer Res 59: 781–786, 1999
65. Wang X, An Z, Geller J, Hoffman RM: A high malignancy orthotopic nude mouse model of the human prostate cancer LNCaP. Prostate 39: 182–186, 1999
66. Kanai T, Konno H, Tanaka T, Matsumoto K, Baba M, Nakamura S, Baba S: Effect of angiogenesis inhibitor TNP-470 on the progression of human gastric cancer xenotransplanted into nude mice. Int J Cancer 71: 838–841, 1997
67. Konno H, Tanaka T, Kanai T, Masuyama K, Nakamura S, Baba S: Efficacy of an angiogenesis inhibitor, TNP-470, in xenotransplanted colorectal cancer with high metastatic potential. Cancer 77(8): 1736–1740, 1996
68. Konno H, Tanaka T, Matsuda I, Kanai T, Maruo Y, Nishino N, Nakamura S, Baba S: Comparison of the inhibitory effect of the angiogenesis inhibitor, TNP-470 and mitomycin C on the growth and liver metastasis of human colon cancer. Int J Cancer 11: 268–271, 1995
69. Konno H, Tanaka T, Baba M, Matsumoto K, Kamiya K, Nakamura S, Baba S, Arai T, Asano M, Suzuki H: Antitumor effect of angiogenesis inhibitors on colon cancer. Biotherapy 11: 993–996, 1997
70. Tanaka T, Konno H, Matsuda I, Nakamura S, Baba S: Prevention of hepatic metastasis of human colon cancer by angiogenesis inhibitor TNP-470. Cancer Res 55: 836–839, 1995
71. Konno H, Arai T, Tanaka T, Baba M, Matsumoto K, Kanai T, Nakamura S, Baba S, Naito T, Sugimura H, Yukita A, As-

ano M, Suzuki H: Antitumor effect of neutralizing antibody to vascular endothelial growth factor on liver metastasis of endocrine neoplasm. Jpn J Cancer Res 89: 933–939, 1998
72. Schabel FM: Animal Models as Predictive Systems in Cancer Chemotherapy Fundamental Concepts and Recent Advances, Year Book Publishers, pp. 323–355, 1975
73. Goldin A, Serpick AA, Mantel N: Experimental screening procedures and clinical predictability value. Cancer Chemother Rep 50: 173–218, 1966
74. Rygaard J, Povlsen CO: Heterotransplantation of a human malignant tumor to "nude" mice. Acta Pathol Microbiol Scan 77: 758–760, 1969
75. Ovejera A: The use of human tumor xenografts in large-scale drug screening. In Kalimann RF (ed) Rodent Tumor Model in Experimental Cancer Therapy, pp 218–220. Pergamon Press, NY, 1987
76. Fidler IJ: Critical factors in the biology of Human Cancer Metastases: twenty Eighth G.H.A Clowes memorial Award Lecture. Cancer Res 50: 6130–6138, 1990
77. Wilmans C, Fan D, O'Brian CA, Bucana CD, Fidler IJ: Orthotopic and ectopic organ environments differentially influence the sensitivity of murine colon carcinoma cells to doxorubicin and 5-fluorouracil. Int J Cancer 52: 98–104, 1992
78. An Z, Jiang P, Wang X, Moossa AR, Hoffman RM: Development of a high metastatic orthotopic model of human renal cell carcinoma in nude mice: Benefits of fragment implantation compared to cell-suspension injection. Clin Exp Metastasis 17: 265–270, 1999
79. Tanizawa A, Fujimori A, Fujimori Y et al.: Comparison of topoisomerase I inhibition, DNA damage, and cytotoxicity of camptothecin derivatives presently in clinical trials. J Natl Cancer Inst 86: 836–842, 1994
80. Cifuentes N, Pickren JW: Metastasis from carcinoma of mammary gland: an autopsy study. J Surg Oncol 11: 193–205, 1979
81. Mundy GR, Yoneda T: Facilitation and suppression of bone metastasis. Clin Orthop 312: 34–82, 1995
82. Guise TA: Parathyroid hormone-related protein and bone metastases. Cancer 80: 1572–1580, 1997
83. Olden K: Human tumor bone metastasis model in athymic nude rats. J Natl Cancer Inst 82: 340–341, 1990
84. Price JE, Polyzos A, Zhang RD, Daniels LM: Tumorigenicity and metastasis of human breast carcinoma cell lines in nude mice. Cancer Res 50: 717–721, 1990
85. Jia T, Liu YE, Liu J, Shi YE: Stimulation of breast cancer invasion and metastasis by synuclein-Γ. Cancer Res 5959: 742–747, 1999
86. Bagheri-Yarmand R, Kourbali Y, Rath AM, Vassy R, Martin A, Jozefonvicz J, Soria C, Lu H, Crepin, M: Carboxymethyl benzylamide dextran blocks angiogenesis of MDA-MB435 breast carcinoma xenograft in fat pad and its lung metastases in nude mice. Cancer Res 59: 507–510, 1999
87. Kurebayashi J, Nukatsuka M, Fujioka A, Saito H, Takeda S, Unemi N, Fukumori N, Kurosumi M, Sonoo H, Dickson RB: Postsurgical oral administration of uracil and tegafur inhibits progression of micrometastasis of human breast cancer cells in nude mice. Clin Cancer Res 3: 653–659, 1997
88. Thompson EW, Brunner N, Torri J, Johnson MD, Boulay V, Wright A, Lippman ME, Steeg PS, Clarke R: The invasive and metastatic properties of hormone-independent but hormone-responsive variants of MCF-7 human breast cancer cells. Clin Exp Metastasis 11: 15–26, 1993
89. Arguello FB, Baggs RB, Frantz CN: A murine model of experimental metastasis to bone and bone marrow. Cancer Res 48: 6876–6881, 1988
90. Sasaki A, Boyce BF, Story B, Wright KR, Chapman M, Boyce R, Mundy GR, Yoneda T: Bisphosphonate risedronate reduces metastatic human breast cancer burden in bone in nude mice. Cancer Res 55: 3551–3557, 1995
91. Morinaga Y, Fujita N, Ohishi K, Tsuruo T: Stimulation of interleukin-11 production from osteoblast-like cells by transforming growth factor-P and tumor cell factors. Int J Cancer 71: 422–428, 1997
92. Guise TA, Yin JJ, Taylor SD, Kumagai Y, Dallas M, Boyce BF, Yoneda T, Mundy GR: Evidence of causal role of parathyroid hormone-related protein in the pathogenesis of human breast cancer-mediated osteolysis. J Clin Invest 98: 1544–1549, 1996
93. Sung V, Gilles C, Murray A, Clarke R, Aaron AD, Azumi N, Thompson EW: The LCC1S-MB human breast cancer cell line expresses osteopontin and exhibits an invasive and metastatic phenotype. Exp Cell Res 241: 273–284, 1998
94. Wang CY, Chang YW: A model for osseous metastasis of human breast cancer established by intrafemur injection of the MDA-MB-435 cells in nude mice. Anticancer Res 17: 2471–2474, 1997
95. Stephenson RA, Dinney CPN, Gohji K, Ordonez NC, Kilion JJ, Fidler IJ: Metastasis model for human prostate cancer using orthotopic implantation in nude mice. J Natl Cancer Inst 84: 951–957, 1992
96. Pettaway CA, Pathak S, Greene G, Ramirez E, Wilson MR, Killion JJ, Fidler IJ: Selection of highly metastatic variants of different human prostatic carcinomas using orthotopic implantation in nude mice. Clin Cancer Res 2: 1627-1636, 1996
97. Saito N, Gleave ME, Bruchovshy N, Rennie PS, Beraldi E, Sullivan LD: A metastatic and androgen-sensitive human prostate cancer model using intraprostatic inoculation of LNCaP cells in SCID mice. Cancer Res 57: 1584–1589, 1997
98. Rembrink K, Romijn JC, van der Kwast TH, Rubben H, Schroder FH: Orthotopic implantation of human prostate cancer cell lines: a clinically-relevant animal model for metastatic prostate cancer. Prostate 31: 168–174, 1997
99. Thalmann GN, Anezinis PE, Chang SM, Zhau HE, Kim EE, Hopwood VL, Pathak S, Eschenbach ACV, Chung WK: Androgen-independent cancer progression and bone metastasis in the LNCaP model of human cancer. Cancer Res 54: 2577–2581, 1994
100. Lin WC, Pretlow TP, Pretlow TG, Culp LA: Bacterial lacZ gene as a highly sensitive marker to detect micrometastasis formation during tumor progression. Cancer Res 50: 2808–2817, 1990
101. Lin WC, Culp LA: Altered establishment/clearance mechanisms during experimental micrometastasis with live and/or disabled bacterial lacZ-tagged tumor cells. Invasion & Metastasis 12: 197–209, 1992
102. Morin J, Hastings J: Energy transfer in a bioluminescent system. J Cell Physiol 77: 313–318, 1972
103. Chalfie M, Tu Y, Euskirchen G, Ward, WW, Prasher DC: Green fluorescent protein as a marker for gene expression. Science 263: 802–805, 1994
104. Cheng L, Fu J, Tsukamoto A, Hawley RG: Use of green fluorescent protein variants to monitor gene transfer and expression in mammalian cells. Nature Biotechnol 14: 606–609,1996

105. Prasher DC, Eckenrode VK, Ward WW, Prendergast FG, Cormier MJ: Primary structure of the Aequorea victoria green-fluorescent protein. Gene 111: 229-233, 1992
106. Yang F, Miss LG, Phillips GN Jr: The molecular structure of green fluorescent protein. Nature Biotechnol 14: 1252–1256, 1996
107. Cody CW, Prasher DC, Welstler VM, Prendergast FG, Ward WW: Chemical structure of the hexapeptide chromophore of the Aequorea green fluorescent protein. Biochemistry 32: 1212–1218, 1993
108. Heim R, Cubitt AB, Tsien RY: Improved green fluorescence. Nature 373: 663–664, 1995
109. Delagrave S, Hawtin RE, Silva CM, Yang MM, Youvan DC: Red-shifted excitation mutants of the green fluorescent protein. Bio/Technology 13: 151–154, 1995
110. Cormack B, Valdivia R, Falkow S: FAGS-optimized mutants of the green fluorescent protein (GFP). Gene 173: 33–38, 1996
111. Zolotukhin S, Potter M, Hauswirth WW, Guy J, Muzycka N: 'Humanized' green fluorescent protein cDNA adapted for high-level expression in mammalian cells. J Virology 70: 4646–4654, 1996
112. Wang X, Fu X, Hoffman RM: A new patient-like metastatic model of human lung cancer constructed orthotopically with intact tissue via thoracotomy in immunodeficient mice. Int J Cancer 51: 992–995, 1992
113. Naumov GN, Wilson SM, MacDonald IC, Schmidt EE, Morris VL, Groom AC, Hoffman RM, Chambers AF: Cellular expression of green fluorescent protein, coupled with high-resolution *in vivo* videomicroscopy, to monitor steps in tumor metastasis. J Cell Sci 112: 1835–1842, 1999
114. Kan Z, Liu T-J: Video microscopy of tumor metastasis: using the green fluorescent protein (GFP) gene as a cancer-cell-labeling system. Clin Exp Meta 17: 49–55, 1999
115. Stewart TA, Pattengale PK, Leder P: Spontaneous mammary adenocarcinomas in transgenic mice that carry and express MTV/myc fusion genes. Cell 38: 627–637, 1984
116. Sinn E, Muller W, Pattengale P, Tepler I, Wallace R, Leder P: Coexpression of MMTV/v-Ha-ras and MMTV/c-myc genes in transgenic mice: synergistic action of oncogenes *in vivo*. Cell 49: 465–475, 1987
117. Guy CT, Cardiff RD, Muller WJ: Induction of mammary tumors by expression of polyomavirus middle T oncogene: a transgenic mouse model for metastatic disease. Mol Cell Biol 12: 954–961, 1992
118. Ritland SR, Rowse GJ, Chang Y, Gendler SJ: Loss of Heterozygosity Analysis in Primary Mammary Tumors and Lung Metastases of MMTV-MTAg and MMTV-*neu* Transgenic Mice. Cancer Res 57: 3520–3525, 1997
119. Guy CT, Webster MA, Schaller M, Parsons TJ, Cardiff RD, Muller, WJ: Expression of the *neu* protooncogene in the mammary epithelium of transgenic mice induces metastatic disease. Proc Natl Acad Sci USA 89: 10578–10582, 1992
120. Leder A, Pattengale PK, Kuo A, Stewart TA, Leder P: Consequences of Widespread Deregulation of the c-*myc* Gene in Transgenic Mice: Multiple Neoplasms and Normal Development. Cell 45: 485–495, 1986
121. Greenberg NM, DeMayo F, Finegold MJ, Medina D, Tilley WD, Aspinall JO, Cunha GR, Donjacour AA, Matusik RJ, Rosen JM: Prostate cancer in a transgenic mouse. Proc Natl Acad Sci USA 92: 3439–3443, 1995
122. Gingrich JR, Barrios RJ, Morton RA, Boyce BF, DeMayo FJ, Finegold MJ, Angelopoulou R, Rosen JM, Greenberg NM: Metastatic prostate cancer in a transgenic mouse. Cancer Res 56: 4096–4102, 1996
123. Gingrich JR, Barrios RJ, Kattan MW, Nahm HS, Finegold MJ, Greenberg NM: Androgen-independent Prostate Cancer Progression in the TRAMP Model Cancer Res 57: 4687–4691, 1997
124. Zhu Y, Richardson JA, Parada LF, Graff JM: Smad3 Mutant Mice Develop Metastatic Colorectal Cancer. Cell 94: 703–714, 1998
125. Donehower LA, Harvey M, Slagle BL, McArthur MJ, Montgomery CA Jr, Butel JS, Bradley A: Mice deficient for p53 are developmentally normal but susceptible to spontaneous tumors. Nature 356: 215–221, 1992

Address for offprints: Robert M. Hoffman, AntiCancer, Inc., 7917 Ostrow Street, San Diego, CA 92111, USA; Fax: 858-268-4175; e-mail: all@anticancer.com